

# Spillover events of rabbit haemorrhagic disease virus 2 (recombinant GI.4P-GI.2) from Lagomorpha to Eurasian badger

Fábio A. Abade dos Santos<sup>1,2,3</sup>  | Andreia Pinto<sup>4</sup>  | Thomas Burgoyne<sup>4,5</sup>  |  
 Kevin P. Dalton<sup>3</sup>  | Carina L. Carvalho<sup>2</sup>  | David W. Ramilo<sup>1</sup>  | Carla Carneiro<sup>1</sup> |  
 Tânia Carvalho<sup>6</sup>  | M. Conceição Peleteiro<sup>1</sup>  | Francisco Parra<sup>3</sup>  |  
 Margarida D. Duarte<sup>1,2</sup> 

<sup>1</sup>Centre for Interdisciplinary Research in Animal Health (CIISA), Faculty of Veterinary Medicine, University of Av. da Universidade Técnica, Lisbon, Portugal

<sup>2</sup>National Institute for Agrarian and Veterinary Research (INIAV, I.P.), Av. da República, Quinta do Marquês, Oeiras, Portugal

<sup>3</sup>Instituto Universitario de Biología de Asturias (IUBA), Departamento de Bioquímica y Biología Molecular, Universidad de Oviedo, Oviedo, Spain

<sup>4</sup>Paediatric Respiratory Medicine, Primary Ciliary Dyskinesia Centre, Harefield NHS Trust, London, UK

<sup>5</sup>UCL Institute of Ophthalmology, University College London, London, UK

<sup>6</sup>Champalimaud Center for the Unknown, Champalimaud Foundation, Lisboa, Portugal

## Correspondence

Fábio A. Abade dos Santos, INIAV  
 IP- National Institute for Agrarian and  
 Veterinary Research, Av. da República,  
 Quinta do Marquês, 2780-157 Oeiras,  
 Portugal.  
 Email: fabio.abade@iniav.pt

## Funding information

Most of the field and laboratory work referred to in this manuscript was supported by Fundação para a Ciência e Tecnologia (FCT; Grant SFRH/BD/137067/2018 and Grant UIDP/CVT/00276/2020) and by Centre for Interdisciplinary Research in Animal Health (CIISA), Faculty of Veterinary Medicine, University of Lisbon (FMV, ULisboa, Portugal). Molecular analysis was funded by Fundo Florestal Permanente (Project + Coelho (Ref 2017014300001) and Project + Coelho 2 (Ref 2019014300001)). FP laboratory was funded by grant AGL2017-83395-R from the Spanish Ministerio de Ciencia Innovación y Universidades, cofinanced by FEDER. Funding bodies played no direct role in the design or conclusion of the study.

## Abstract

Rabbit haemorrhagic disease (RHD) is a major threat to domestic and wild European rabbits. Presently, in Europe, the disease is caused mainly by Rabbit haemorrhagic disease virus 2 (RHDV2/b or *Lagovirus europaeus* GI.2), the origin of which is still unclear, as no RHDV2 reservoir hosts were identified. After the RHDV2 emergence in 2010, viral RNA was detected in a few rodent species. Furthermore, RHDV2 was found to cause disease in some hare species resembling the disease in rabbits, evidencing the ability of the virus to cross the species barrier. In this study, through molecular, histopathologic, antigenic and morphological evidences, we demonstrate the presence and replication of RHDV2 in Eurasian badgers (*Meles meles*) found dead in the district of Santarém, Portugal, between March 2017 and January 2020. In these animals, we further classify the RHDV2 as a *Lagovirus europaeus* recombinant GI.4P-GI.2. Our results indicate that *Meles meles* is susceptible to RHDV2, developing systemic infection, and excreting the virus in the faeces. Given the high viral loads seen in several organs and matrices, we believe that transmission to the wild rabbit is likely. Furthermore, transmission electron microscopy data show the presence of calicivirus compatible virions in the nucleus of hepatocytes, which constitutes a paradigm shift for caliciviruses' replication cycle.

## KEYWORDS

Eurasian badger, GI.2, *Meles meles*, recombinant GI.4P-GI.2, RHDV2/b, spillover event

## 1 | INTRODUCTION

Rabbit haemorrhagic disease virus 2 (RHDV2, also referred to as *Lagovirus europaeus* GI.2 or RHDVb (Le Pendu et al., 2017)) is a highly contagious *Lagovirus* of the *Caliciviridae* family that causes an acute infection in wild and domestic European rabbits (*Oryctolagus cuniculus*).

The virion measures from 27 to 40 nm (Capucci et al., 1991; Ohlinger et al., 1990) in diameter with the icosahedral typical morphology of the *Caliciviridae* and a surface consisting of regularly arranged, cup-shaped depressions (Capucci et al., 1991; Ohlinger et al., 1990). The genomic material is composed of a single-stranded, non-segmented, positive-sense RNA genome of 7,437 nucleotides (Meyers et al., 1991). Also, the virus contains a sub-genomic 2.2 kb RNA, collinear to the 3' region of the genome (Ohlinger et al., 1990).

RHDV2 emerged in 2010 in France (Le Gall-Recule et al., 2011) and rapidly replaced the former circulating RHDV classical strains (GI.1) in several European countries, also expanding to many regions in the world (Mahar et al., 2018). Since 2012, no RHDV GI.1 strains (former G1 to G6) have been reported in the Iberian Peninsula. Furthermore, following the detection of RHDV2 strains, recombinant strains containing the non-structural region of GI.1 or non-pathogenic RHDV strains (GI.3 and GI.4) and the structural region of RHDV2 (GI.2) strains were identified. Several recombination breaking points have been described (Silvério et al., 2018). Of these, the recombinant hotspot located at the RdRp/VP60 level seems to play an important role in the evolution of the new variants (Abrantes et al., 2020; Dalton et al., 2018; Silvério et al., 2018).

Another member of the *Lagovirus* genus, the rabbit calicivirus (RCV, GI.5; Capucci et al., 1996) is an asymptomatic virus of the intestinal tract. In addition to these, the European RCV-E1 (GI.3) and Australian RCV-A1 (GI.4; Le Gall-Reculé et al., 2011; Strive et al., 2009) are non-pathogenic rabbit viruses. The information on these viruses is scarce but can contribute as genetic donors resulting in recombinant pathogenic viruses (Silvério et al., 2018).

Other than in the domestic and wild rabbit, RHDV2 has also been reported in several hare species, namely the Sardinian Cape hare (*Lepus capensis mediterraneus*; Puggioni et al., 2013), the Italian hare (*Lepus corsicanus*; Camarda et al., 2014), the European brown hare (*Lepus europaeus*; Velarde et al., 2017) and the Mountain hare (*Lepus timidus*; Neimanis et al., 2018) and recently in the jackrabbit (*Lepus californicus*; USDA, 2020), desert cottontails (*Sylvilagus audubonii*; USDA, 2020) and eastern cottontail (*Sylvilagus floridanus*; USDA, 2020), causing haemorrhagic disease similar to that of the European rabbit.

The concomitant ability of RHDV2 to infect hares, alongside with the high fatality rates in both young and adult rabbits (Le Gall-Recule et al., 2011), contrasts the epidemiological and pathological pattern of RHDV GI.1, which affects only rabbits older than 4 weeks of age (Liu et al., 1984), although there is isolated evidence of RHDV-RNA presence in hares (Lopes et al., 2014).

In areas where RHDV2 circulates, sympatric Iberian meso-carnivores come in contact with the virus, either by predation or

necrophagy of infected leporids or through contact with contaminated soil or vegetation (OIE, 2019). RHDV2-RNA was identified in pine voles (*Microtus pinetorum*) and white-toothed shrews (*Crocidura russula*), two rodent species that are sympatric to the European wild rabbit (Calvete et al., 2019). The RHDV2 transmission to small mammals could happen due to their scavenging habits, or by ingestion of rabbit infected tissues or faeces (Calvete et al., 2019). Additionally, it is also known that red foxes (*Vulpes vulpes*; Chiari et al., 2016) and wolf (*Canis lupus*; Di Profio et al., 2017) play a role as passive carriers of lagoviruses, spreading European brown hare syndrome virus (EBHSV) by their faeces after ingestion of infected hares.

Given this possibility, several sympatric species of wild animals have been investigated for RHDV2 at our laboratory over the last three years (data not shown), namely birds, rodents and carnivores, including mustelids such as the Eurasian badger. The Eurasian badger (*Meles meles*) is a gregarious, fossorial, and evasive species. Badgers are predominantly nocturnal or crepuscular (Fedriani et al., 1999), mainly in the spring, when the wild rabbit activity peak coincides with the peak of RHD (Mutze et al., 2002). This trophic, opportunistic, generalist species preys on the European rabbit, particularly juvenile (Fedriani et al., 1999). In the summer and autumn/winter, lagomorphs represent about 60% and 22.7% of a badger's diet, respectively (Fedriani et al., 1999), whereas in the spring rabbit may account for up to 87.9% of the ingested biomass according to a study carried out in Spain (Fedriani et al., 1999).

This study was part of a three years monitoring programme to investigate haemorrhagic disease in the wild rabbits and sympatric species collected in mainland Portugal. Among several non-leporid species investigated, some of the badgers tested RHDV2 positive by molecular methods. This finding prompted us to further investigate the presence of RHDV2 proteins, viral particles and RHDV2 compatible lesions in this species. To our knowledge, we are reporting for the first time the *Lagovirus europaeus* GI.4P-GI.2 crossing the barrier beyond the Lagomorpha order, namely to the Eurasian badger.

## 2 | MATERIALS AND METHODS

### 2.1 | Origin of the animals

A total of 10 European badgers were admitted for this study. All the information collected about these animals, namely sex, weight and date of collection, among others, is summarized in Table S1.

One badger (B1) found dead on the road and nine others (B2 to B10) found dead in agricultural areas were collected during active prospection for wild rabbit carcasses and sympatric species, namely foxes, insects, birds and rodents, within the scope of an epidemiological evaluation of haemorrhagic disease in rabbit populations. All badger carcasses were found in the District of Santarém (Portugal NUT III, PT185 area).

The poor quality of the wildlife biological samples posed a major challenge to the laboratory diagnosis, which was overcome through the establishment of a comprehensive diagnosis strategy resourcing

to several molecular, antigen detection methods, sequencing and transmission electron microscopy (TEM). Thus, the methodological strategy adopted was as follows: samples were tested by RT-qPCR (Duarte et al., 2015) and the negatives were excluded from further analyses. The RT-qPCR-positive badgers showing milder autolysis were selected for RHDV2 sequencing analysis, immunohistochemistry (IHC) and TEM.

## 2.2 | Necropsy sampling and histopathology

B1 was maintained at  $-20^{\circ}\text{C}$  until necropsy, while the remaining carcasses were kept at  $4^{\circ}\text{C}$  for a maximum period of 2 days. No badger was necropsied along with other species, namely rabbits, to avoid cross-contaminations. Necropsies were performed according to the routine implemented practices, as described in the necropsy manual (Peleteiro et al., 2016), and carried out at the Faculty of Veterinary Medicine, University of Lisbon (FMV-ULisboa, Lisbon, Portugal) or at the National Institute for Agricultural and Veterinary Research (INIAV I.P., Oeiras, Portugal).

Different samples were collected for molecular diagnosis, histopathology and bacteriology. To avoid faecal contamination, the sample collection was carried out in the following order: liver, spleen, kidney, lung, left ventricle, other organs, duodenum and finally faeces. Disposable material was used for each organ to avoid cross-contamination between matrices. Blood samples were not collected due to coagulation and/or autolysis.

For histopathology, liver, spleen, duodenum, stomach, kidney, lung, left ventricle, trachea and mesenteric lymph nodes were collected and fixated in 10% (v/v) neutral buffered formalin, routinely paraffin-embedded, sectioned at  $3\ \mu\text{m}$  and stained with haematoxylin and eosin (H&E). Microphotographs were obtained with a DP23 Olympus digital camera.

Perls Prussian Blue was used to detect the presence of non-haem iron (ferritin and haemosiderin) in the tissues (Bancroft & Stevens, 1990).

## 2.3 | Immunohistochemistry and dot blotting

Immunohistochemistry was performed as follows: (a)  $4\ \mu\text{m}$  sections of liver samples were mounted in appropriated glass slides; (b) deparaffinization and antigen retrieval were performed in a PT Link (Dako) at  $96^{\circ}\text{C}$  for 20 min, with low pH EnVision FLEX target retrieval solution (code DM829; Dako); (c) peroxidase block (with Peroxidase blocking solution, DAKO) was carried out for 20 min at room temperature; (d) primary antibody (named pAb or Virlab derived from a hyperimmune serum collected from a rabbit infected in the facilities of the University of Oviedo (UniOvi) with strain RHDV-Ast89 (RHDV)), diluted at the optimized concentration (1/1000) in Antibody Diluent (DAKO), was incubated for 1 hr at room temperature; (e) incubation with the secondary antibody (at the concentration indicated by the manufacturer (Dako EnVision™+ Dual Link System-HRP, mouse

anti-rabbit)), for 30 min at room temperature; (f) staining with DAB chromogen (DAKO) for 5 min; (g) nuclei counterstain with Gills haematoxylin and finally (h) dehydration in an ethanol gradient. Finally, the sections were mounted with a non-aqueous mounting medium. The necessary washes between incubations were performed with phosphate-buffered saline, pH 7.4 (PBS) twice for 5 min each with frequent manual agitation. The pAb was previously validated against RHDV and RHDV2 (González, 2019).

Dot blot was carried out using approximately 20% (w/v) homogenates prepared in PBS of liver and lung samples from badgers B5 and B6 after clarification at  $6,000\ g$  for 5 min. Liver homogenates from RHDV2-positive and RHDV2-negative rabbits were used as positive and negative controls, respectively. A grid was drawn on a piece of nitrocellulose membrane (Thermo Fisher Scientific Inc.) using a pencil.  $1\ \mu\text{l}$  drops were deposited in the middle of the squares, and the membrane was allowed to dry for 15 to 20 min at room temperature. The inhibition of non-specific reactions was performed by shaking incubation with 5% milk powder in PBS (w/v) for 45 min at room temperature. Two 5-min washes with shaking were performed with 0.05% Tween 20 (v/v) in PBS. Then, the membranes were incubated for 1h at room temperature with agitation with primary antibodies diluted at the optimized concentrations in 0.05% Tween 20 in PBS. Two monoclonal antibodies (mAb) were used, namely 1A2 (anti-VP60, Ingenasa) and 3A10 (anti-VP60 of RHDV and RHDV2, S domain, produced in the Department of Biochemistry and Molecular Biology (UniOvi)). The polyclonal antibody (pAb) was also used. After incubation, two additional washes were performed as described above. The membranes were then incubated in the dark under shaking conditions with the secondary antibody, goat anti-rabbit IgG, conjugated with fluorescein isothiocyanate (FITC; Merck Life Science S.L.U. suc) for the polyclonal serum or anti-Mouse IgG (whole molecule)—FITC antibody produced in goat (Sigma-Aldrich) for the monoclonal antibodies, both diluted at 1:200 in PBS-Tween (0.05% Tween 20 (v/v) in PBS) for 1 hr, at room temperature. Finally, after two wash steps of 5 min each, visualization of membranes was carried out using Odyssey Infrared Imaging System (LI-COR Biosciences) and the software Image Studio (LI-COR Inc.).

## 2.4 | Immunofluorescence

Tissue samples from B5 and B6 were embedded in optimal cutting temperature (OCT) compound, and sections were cut onto slides using a cryostat at  $-20^{\circ}\text{C}$ . The cryostat sections were permeabilized using 0.2% saponin in PBS (w/v) for 20 min before emerged in blocking solution (0.02% saponin, 1% BSA in PBS) for 30 min at room temperature. Antibody labelling was performed by incubating sections with pAb (polyclonal antibodies) and the mouse monoclonal anti-LAMP1 antibody (ab25630, Abcam) in blocking solution for 2 hr at room temperature. Secondary antibodies used at 1:500 (Goat anti-Rabbit IgG (H + L) cross-adsorbed secondary antibody, Alexa Fluor 488 (ThermoFisher A-11008) and goat anti-mouse IgG (H + L) cross-adsorbed secondary antibody, Alexa

Fluor 555 (ThermoFisher A-21422)) and in some cases, fluorescent phalloidin (ab176759, Abcam), were added to the sections and incubated for 1 hr at room temperature. Finally, coverslips were added to the slides using mounting media containing DAPI (ab228549, Thermo Fisher Scientific Inc.). Images were acquired in a Leica SP8 confocal microscope, and greyscale inverted images were produced using ImageJ (NIH). Negative controls were either uninfected or infected samples where the polyclonal antibody was omitted.

## 2.5 | Molecular diagnosis of RHDV, sequencing and phylogenetic analysis

The tissue and faeces samples were homogenized at 20% in sterile PBS (w/v), using mechanical homogenization with 0.5 mm zirconium beads (Sigma-Aldrich) and the FastPrep FP120 Bio101 Homogenizer (Level 5 velocity, 45s, Savant Instruments). Total nucleic acids were extracted from 200  $\mu$ l supernatant after a 5 min 6,000g centrifugation. The automatic extraction was performed with the MagAttract 96 cadour Pathogen kit (Qiagen) on the BioSprint 96 automatic extractor, following the protocol supplied with the kit.

Each tissue and faecal sample was tested for RHDV2-RNA (GI.2) by a specific RT-qPCR developed by Duarte et al. (2015) that targets a 127 nt region of the VP60 gene, using the OneStep RT-PCR Kit (Qiagen).

cDNA was synthesized with the SuperScript™ IV First-Strand Synthesis System (Invitrogen) according to the manufacturer's recommendations, using either oligo(dT)<sub>12-18</sub> and random hexamers.

The conventional RT-PCR (Dalton et al., 2018) for differentiation of RHDV2 strains from RHDV2 recombinants was carried out using the Phusion Flash High-Fidelity PCR Master Mix (Thermo Fisher Scientific Inc.) according to the manufacturer's recommendations.

For two positive liver samples (B5 and B6), amplification of the partial RdRp gene and full VP1 (VP60) gene sequence was accomplished using the primers described in Table S2, where all the primers used in this investigation are shown. Regarding the other samples, partial sequencing (Table S1) was performed to confirm the presence of RHDV2.

The amplicons were purified using the NZY GelPure kit (NZYTech), following the manufacturer's instructions, and directly sequenced with a 3130 Genetic Analyser (Applied Biosystems). The resulting sequences were analysed using Seqscape software v2.7 (Applied Biosystems). Merged and assembled consensus sequences were submitted to GenBank.

The partial sequence of RNA polymerase (RdRp) gene and the complete vp60 gene sequence from badger B6 were compared with reference strains for all known RHDV and RHDV2 genotypes, and variants that infect the European rabbit for which this genomic region are available in the database. The accession numbers are shown in the phylogenetic tree (Figure 16). The alignment was achieved

using the Mega X, for a total of 2,191 positions (partial RdRp gene and complete VP60 gene) and the evolutionary history inferred using the Maximum Likelihood method and General Time Reversible model (Nei & Kumar, 2000). The model was selected using the Mega Function having selected the model GTR + G+I (BIC 37184.06 and AIC 36028.07).

The known principal genotypes and variants of *Lagovirus* that can infect the *Oryctolagus cuniculus* are shown in the figure, as reference. The tree with the highest log likelihood (-17929.21) is shown.

## 2.6 | Transmission electron microscopy

Transmission electron microscopy (TEM) was performed in liver samples from three badgers (B1, B5 and B6). Briefly, samples were fixed for 72 hr with a solution 0.1 M sodium cacodylate (Sigma-Aldrich) containing 2.5% glutaraldehyde (Sigma-Aldrich). The regions of interest were sliced in small ~1 mm<sup>3</sup> and washed five times in 0.1 M sodium cacodylate buffer, and samples were then post-fixed with 1% osmium tetroxide (EMS) for 1 hr, and en bloc stained with 1% Millipore-filtered uranyl acetate (Agar Scientific). Samples were dehydrated in increasing concentrations of ethanol, infiltrated and embedded in EPON 812 (EMS). Polymerization was performed at 60°C for 24 hr, and ultrathin sections were obtained in a Reichert ultracut E ultramicrotome (Leica), collected to 1% formvar-coated copper slot grids (Agar Scientific), stained with 2% aqueous uranyl acetate and lead citrate and examined in a Jeol 1400 plus transmission electron microscope at an accelerating voltage of 120 kV. Digital images were obtained using an AMT XR16 bottom mid mount digital camera (AMT). The sections were systematically analysed using AMT© software and several high and low magnifications were acquired.

## 2.7 | Other virological analyses

Tissue and faeces samples were homogenized and total nucleic acids extracted as described above. Feline and canine Parvoviruses, canine distemper virus (morbillivirus), mammal (canine, feline and porcine) coronaviruses, type A rotavirus, Ausjesky disease virus and other herpesviruses were investigated using the methods and matrices described in Table S3.

## 2.8 | Bacteriological analysis

Liver, spleen, kidney and lung from B5, B6, B7 and B8 badgers were collected at necropsy for bacteriology using conventional techniques. In the case of B5 and B6, all samples were processed separately. A pool of organs from the animal was prepared for B7 and B8. The remaining badgers were not sampled for bacteriology due to extensive autolysis or faecal contamination.

Briefly, aerobic bacteria isolation was performed on Columbia agar supplemented with 5% sheep blood (BioMérieux) and MacConkey agar (Thermo Fisher Scientific Inc.), incubated at 37°C for 24 to 48 hr. Strict anaerobic bacteria isolation was performed on Schaedler agar supplemented with 5% sheep blood (BioMérieux) and incubated for 48 hr at 37°C in the absence of oxygen. Afterwards, isolates were identified through their macro- and microscopic morphology, staining characteristics and biochemical profiling using API (BioMérieux) galleries, according to the manufacturer's instructions.

## 2.9 | Parasitological analysis

Faeces were collected for the flotation method to detect helminth eggs or protozoan oocysts. Faeces were mixed with saturated sugar solution (1:4), and after pouring the solution into tubes, lamellae were placed on their top to allow adhesion to the glass and allowed to stand for 15 min. Lamellae were then transferred to slides, and preparations were observed with a compound microscope.

Gastrointestinal content was also collected and placed on a tray with a black background, filled with warm water and, after standing for a few minutes, supernatant was removed by decantation. This procedure was repeated three times until the liquid became clear enough to visualize the presence of helminths by contrast. Furthermore, flotation method for egg and oocyst detection was also performed as described above.

## 3 | RESULTS

### 3.1 | Necropsy data

Necropsy of badger B1 revealed a good overall body condition, multiple fractures of the skull and lacerations in the liver and spleen, interpreted as resulting from a traffic accident. The autolysis limited the interest in the identification of the lesions, both grossly and microscopically. B2, B3, B4, B9 and B10 presented severe autolysis, good body condition and no visible lesions. Badgers B5 and B6 were emaciated, severely dehydrated, with uncoagulated blood, congestive foci in the lungs and slightly discolored liver. B7 and B8 presented similar lesions, however with coagulated blood. Other data from the necropsies are shown in Table S1 available as supplementary data.

### 3.2 | Histopathological findings

Histopathology data for badgers B5 to B8 are summarized in Table 1, and the main findings shown in Figures 1 to 10.

Liver of 3 out of 4 badgers showed areas of hepatocellular hydropic degeneration and individual cell necrosis (Figures 1 and 2). In two cases (B7 and B8), generalized moderate oedema of the

perisinusoidal space (space of Disse) was evident. Kupffer cells containing haemosiderin were identified in B8.

Spleen showed haemosiderin-laden macrophages in the red pulp in most cases. This was marked in badgers B5 and B8, posteriorly demonstrated with Perls Blue stain for iron (Figure 3) and mild to moderate in all others. In two badgers (B5 and B6), white pulp hyperplasia was also seen (Figure 4). In one case (B8), not coincident with the lymphoid hyperplasia, focal deposits of acidophilic material (fibrin-like) were present in germinal centres (Figure 5).

In the lungs, severe congestion of interalveolar septa was present in badger B6 and B7 (Figure 6). Small aggregates of haemosiderin-containing macrophages were detected in the interalveolar septa in one case (B6) (Figure 7). In two badgers, interalveolar septa were thickened due to marked to moderate infiltration of mononuclear inflammatory cells (diffuse interstitial pneumonia; Figure 8).

In the kidneys, vacuolar and granular degeneration of tubular cells in the proximal and distal tubules was present in all cases. In some of these tubules, necrosis of tubular cells was evident. In the heart, cardiomyocyte degeneration consisting of loss of striation and granular appearance of the cytoplasm was evident (Figure 9). In one case (B6), this was accompanied by focal haemorrhage (Figure 10).

### 3.3 | Immunohistochemistry and Dot blot

To investigate the presence of the virus in the tissues, detection of the viral capsid protein (mainly composed by VP60) was attempted in badger and rabbit tissues by immunolabelling techniques using polyclonal (pAb) against RHDV and monoclonal antibodies (1A2 and 3A10).

Immunohistochemistry of badgers' livers carried out with the pAb allowed the observation of generalized cytoplasmic staining of the hepatocytes of badgers B5 (Figure 11) and B6 (showing similar staining, result not shown), contrarily to the absence of staining in liver samples from a qPCR-negative badger and a qPCR-negative rabbit (results not shown). In addition to cytoplasmic staining in badgers B5 and B6, some hepatocytes also showed nuclear staining.

The same positive reaction for badgers B5 (weaker) and B6 (stronger) was observed in the dot blot analyses (Figure 12). Like in immunohistochemistry, in the dot blot, the pAb generated stronger reactions.

### 3.4 | Immunofluorescence

To further demonstrate replication of RHDV2, indirect immunofluorescence was performed in the liver of badgers B5 and B6 (named #1 and #2, respectively, in Figure 13). We observed encapsulated virions, recognizable by the FITC antibody directed to VP60, whose density is compatible with active replication of RHDV2 in the tissues (Figure 13). DAPI staining was used for labelling DNA in fluorescence microscopy and phalloidin to stain the actin filaments. Livers from an RHDV2-infected rabbit and the RHDV2 non-infected badger were used as a positive and negative control, respectively.

**TABLE 1** Histopathological findings in badgers B5, B6, B7 and B8

ID	Liver	Spleen	Lung	Kidney	Others
B5	Hepatocytes with minimal changes. In some areas, they show mild hydropic degeneration.	Accumulation of haemosiderin-laden macrophages in the red pulp. Mild hyperplasia of lymphoid follicles, which show foci of acidophilic material compatible with fibrin in the germinal centres.	Thickening of interalveolar septa with infiltration by mononuclear inflammatory cells (diffuse interstitial pneumonia). Frequent aggregates of haemosiderin-laden macrophages. Vicarious alveolar emphysema. Shrinked pleura.	Vacuolar and granular degeneration of epithelial cells in the proximal and distal tubules.	Cardiomyocytes granular degeneration and loss of striation. Thymus: necrosis of 10%–15% of lymphocytes, which show karyolysis and karyorrhexis.
B6	Severe congestion. Hepatocytes with generalized and severe hydropic degeneration. About 50% of the hepatocytes show no nucleus (karyolysis).	Hyperplasia of lymphoid follicles. Diffuse infiltration of red pulp by mononuclear cells (chronic splenitis).	Severe congestion and moderate thickening of alveolar septa by mononuclear inflammatory cells (interstitial pneumonia). Frequent aggregates of haemosiderin-laden macrophages. Vicarious alveolar emphysema.	Congestion of the cortex. Necrosis of tubular epithelium of proximal and distal tubules.	Cardiomyocytes granular degeneration and loss of striation. Haemorrhagic foci.
B7	Occasional hyperchromatosis of the nuclear membrane, karyorrhexis and pycnotic nuclei. Space of Disse oedema with mild atrophy of hepatocytes.	Lymphoid follicles hypoplasia and fibrotic changes of the red pulp (chronic splenitis).	Severe congestion and moderate thickening of alveolar septa by mononuclear inflammatory cells (interstitial pneumonia). Vicarious alveolar emphysema.	Vacuolar and granular degeneration of epithelial cells in the proximal and distal tubules.	Cardiomyocytes granular degeneration and loss of striation.
B8	Generalized hepatocyte hydropic degeneration. Occasional hyperchromatosis of the nuclear membrane, karyorrhexis and pycnotic nuclei. Intralobular Kupffer cells containing haemosiderin. Space of Disse oedema.	Accumulation of haemosiderin-laden macrophages in the red pulp. Lymphoid follicles show small deposits of acidophilic material compatible with fibrin in the germinal centres together with haemosiderin-laden macrophages.	Thickening of interalveolar septa with infiltration by mononuclear inflammatory cells (diffuse interstitial pneumonia).	Vacuolar and granular degeneration of epithelial cells in the proximal and distal tubules.	Cardiomyocytes granular degeneration and loss of striation.

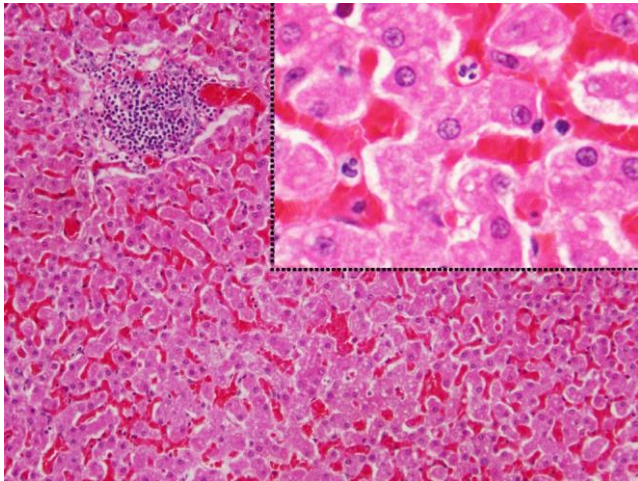


**FIGURE 1** Liver (B6). Mild hydropic degeneration of the hepatocytes in the lower centre. Focal infiltration of mononuclear cells in the upper left. The hydropic degeneration can be seen at higher magnification in the inset. H&E,  $\times 100$ , inset,  $\times 400$

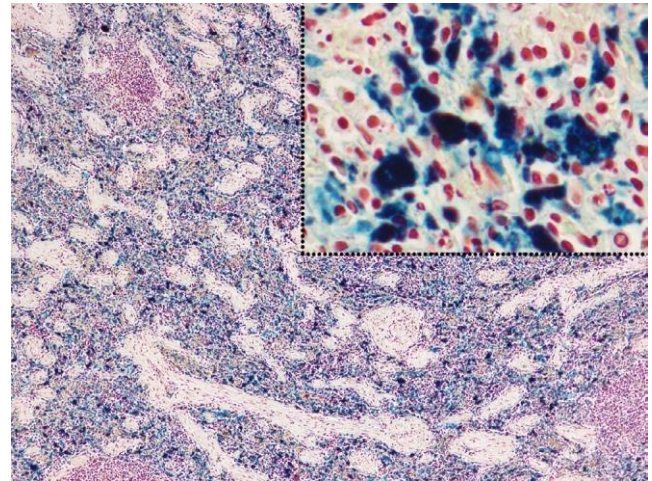


**FIGURE 3** Spleen (B8). Marked presence in the red pulp of haemosiderin containing macrophages. Perls Blue,  $\times 40$ , inset  $\times 100$

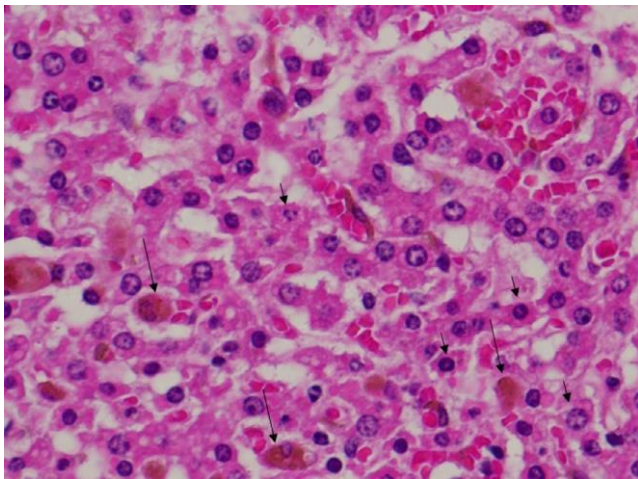


**FIGURE 2** Liver (B8). Hydropic degeneration of the hepatocytes. Some cells show pyknosis and karyorrhexis (short arrows), as well as hyperchromatosis of the nuclear membrane; oedema of the perisinusoidal space and Kupffer cells containing haemosiderin (long arrows). H&E,  $\times 400$

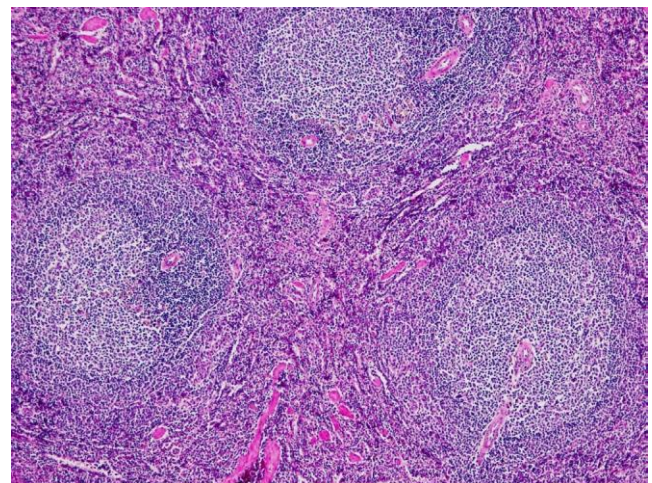


**FIGURE 4** Spleen (B6). Hyperplasia of the lymphoid follicles. H&E,  $\times 100$

A clear green labelling is observed in both badgers' livers and in the RHDV-2 positive rabbit sample. The badgers' samples showed distinct punctate staining (more evident in the B6), ascribing virus localization to subcellular compartments. Due to the poor tissue preservation conditions, DAPI is dispersed by the cytoplasm of cells. For the same reason, phalloidin is sometimes also difficult to observe.

To evaluate the presence and increment of lysosomal or autophagosome-like structures that are usually associated with viral factories, LAMP 1 fluorescence staining was performed. The membrane glycoprotein 1 was detected by direct immunofluorescence (Figure 14a) in the cytoplasm of infected hepatocytes. The presence of a large number of lysosomes was also confirmed in hepatocytes

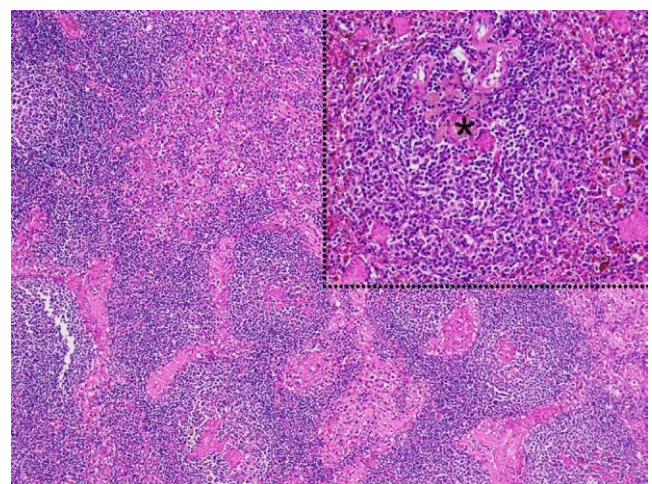


**FIGURE 5** Spleen (B8). The centre of some lymphoid follicles shows focal deposits of acidophilic material (\*). H&E,  $\times 40$ , inset  $\times 100$

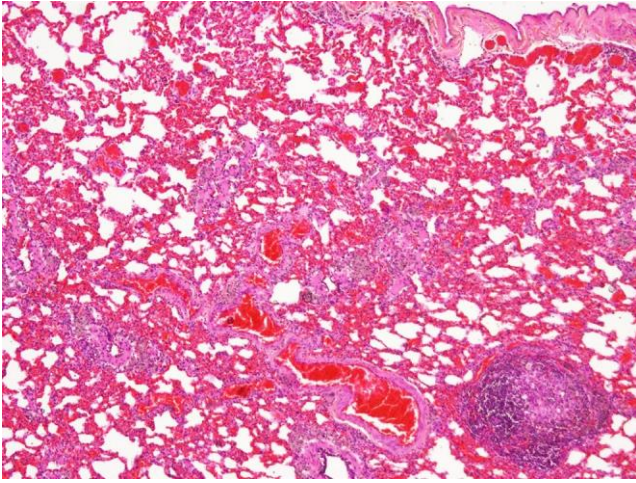


**FIGURE 6** Lung (B6). Severe diffuse congestion of the alveolar septa some of which are thickened due to inflammatory cell infiltration. Granuloma in the lower right. H&E,  $\times 40$

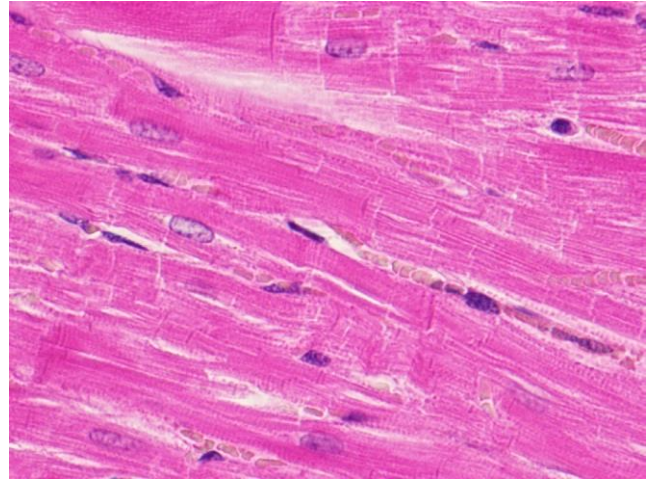


**FIGURE 9** Myocardium (B5). Striation loss and granular appearance of the cardiomyocytes. H&E,  $\times 400$

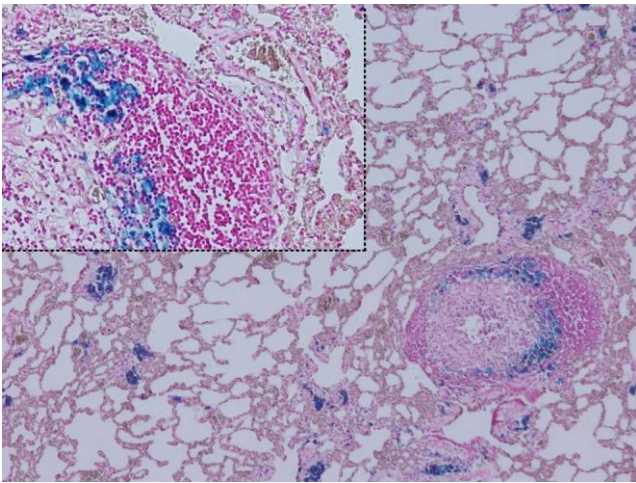


**FIGURE 7** Lung (B6). Iron deposits in the alveolar septa and in macrophages in the periphery of a granuloma. Perls Blue,  $\times 40$ , inset  $\times 100$

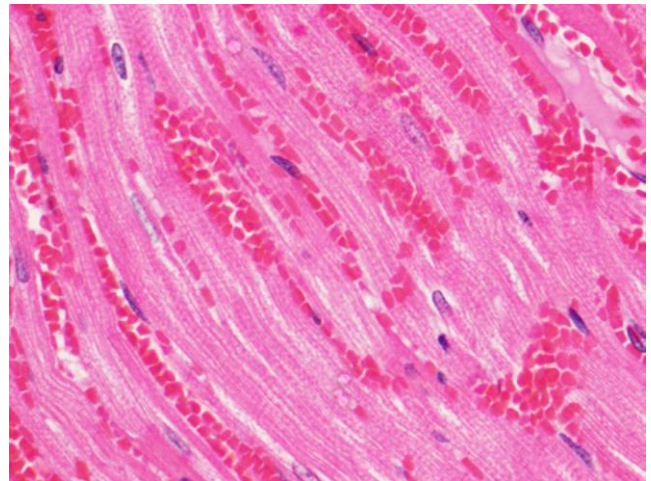


**FIGURE 10** Myocardium (B6). Focal intercellular haemorrhage. Striation loss and granular appearance of the cardiomyocytes. H&E,  $\times 400$

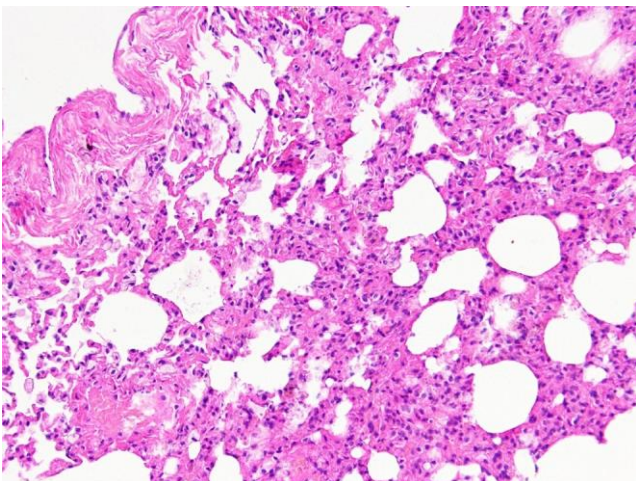


**FIGURE 8** Lung (B8). Diffuse interstitial pneumonia. The pleura is corrugated. H&E,  $\times 100$

of RHDV2-infected badgers (B1, B5 and B6) by TEM showing that viral particles colocalize with lysosomal structures, indicating that the virus is within lysosomes (Figure 14b,c).

### 3.5 | Molecular diagnosis and sequencing analysis

RHDV2-RNA was detected by RT-qPCR in most of the organs from badgers B1, B5–B10 (Table 2), suggesting that the virus was disseminated systemically. In general, the higher viral loads were observed in the liver and spleen (Table 2). None of the badgers tested positive for RHDV GI.1-RNA.

Full RHDV2 vp60 sequences were obtained for badgers B5 and B6 showing these to be RHDV2 strains (GI.2). Despite RHDV2 vp60 genes from badgers B1, B7 to B10 vp60 genes not being sequenced, given the specificity of the RT-qPCR method used for

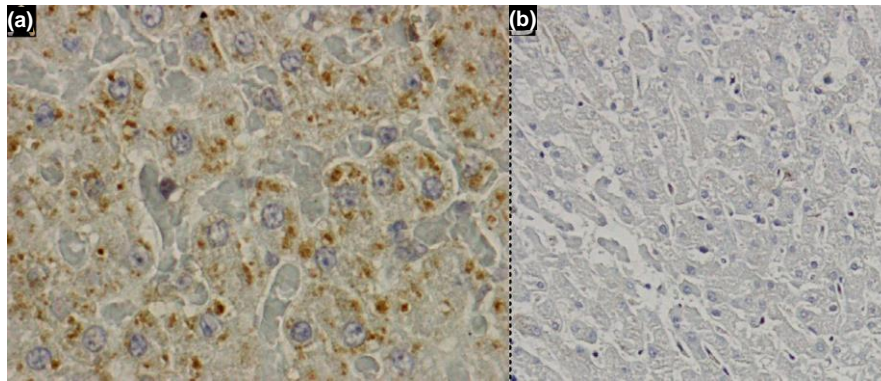


**FIGURE 11** Immunostaining for RHDV2 in the liver of badger B5 (left). Hepatocytes show cytoplasmic granular brown staining. At right, negative control of a non-infected badger liver. DAB counterstained with Gills haematoxylin,  $\times 400$

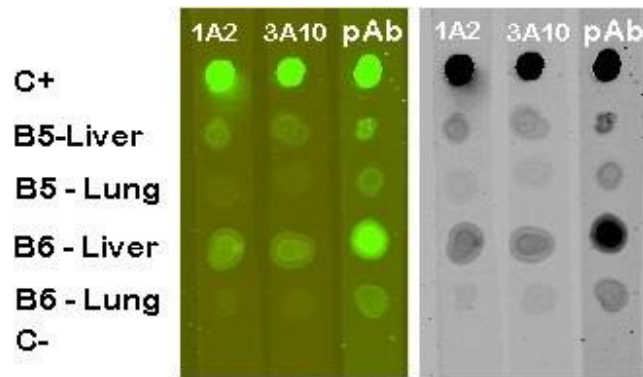


**FIGURE 12** Dot blots from B5 and B6 badgers. C + homogenate from a RHDV2-positive rabbit. C - Bovine serum albumin

RHDV2 (Duarte et al., 2015) detection to which they were positive, allowed to conclude that the strains from these badgers were also GI.2.

To further investigate the genomic composition of the RHDV2 badgers' strains, an upstream genomic region comprising the 3' end of the RdRp gene was amplified by a conventional RT-PCR (Dalton et al., 2018) and sequenced.

The partial RdRp nucleotide sequences from badgers B1(MW446907), B5(MT610362), B6(MT610363), B7(MW446908), B8(MW446909) and B9(MW446910) showed higher identity to GI.4 strains regarding this non-structural gene.

The final RdRp/VP60 2,188 nucleotide sequences obtained from badger B5 (MT610362) and badger B6 (MT610363) were aligned and compared, showing 100% identity with each other. BLAST search (performed on 5th January 2021) using the VP60 sequence showed higher similarities, namely 99.37% and 98.10% with MG763954 (a recombinant strain reported in 2018 from a wild rabbit collected in Estremoz, south Portugal), and KF442963 (also a recombinant strain obtained in 2013 from a wild rabbit from in Barrancos, south Portugal), respectively. The BLAST analysis of the RdRp partial sequences of B5 and B6 showed higher identity with the same sequences, namely 97.54% with sequence MG763954.

The partial RdRp nucleotide sequences (409nt long) from badgers B5 and B6 shared 95% of identity with B1, 83% with B7 and B8, and 82% of identity with B9.

The amino acid sequence of the partial RdRp (149 residues long) deduced from sequence MT610363 (B5) showed 98.66% identity

with the homologous region from sequence AIT40572.2 (RHDV2 collected from a wild rabbit from Estoi, Faro, south of Portugal in 2013). Also, the complete amino acid sequence of VP60 gene (579 residues long) deduced from sequence MT610363 showed 99.83% identity with the VP60 sequence from a strain collected from Valpaços, Vila Real Portugal in 2012 (AJE29738).

When the deduced amino acid (aa) sequences comprising the contiguous partial RdRp gene and the complete VP60 gene were compared with the sequences available in the GenBank database, the greatest identity (99.59%) was found with sequence AIT40572.2. With regards to this sequence, three aa substitutions were observed in the RHDV2 badger sequence MT610363, namely an Ala<sup>1648</sup> to Thr<sup>1648</sup> (a radical aa residue change) and a Tyr<sup>1737</sup> to His<sup>1737</sup> (conservative replacement) located in the RdRp protein, and one substitution in the VP60 protein, namely a Thr<sup>2109</sup> to Ser<sup>2109</sup> (conservative replacement), located in loop L2 of P2 sub-domain (positions indicated refer to the polyprotein). These three aa residues found in the B5 and B6 RHDV2 polyprotein are not unique in badgers' strains, being also found in rabbits' strains.

### 3.6 | Phylogeny of the badgers' RHDV2 strains

The 2,191-nt long region containing the partial RdRp gene and full VP1 (VP60) gene sequences from badger B5 (MT610362) and B6 (MT610363) was used to assess the phylogenetic relationships between these strains and the RHDV and RHDV2 strains from wild rabbits by maximum likelihood (ML; Figure 15).

As expected, the RHDV2 badger strains, represented by sequence MT610363, were grouped with Portuguese recombinant RHDV2 strains, close to the reference strain RCV-A1-like/RHDV2 (MG763954), with variant of GI.4 of polymerase gene and GI.2 VP60 genotype. The access numbers of the sequences included in the tree are shown in the phylogenetic tree (Figure 15).

### 3.7 | Transmission Electron Microscopy

Viral particles were identified by transmission electron microscopy (TEM) in liver of badgers B1, B5 and B6. Virions showed the typical icosahedral morphology and size was of  $33.4 \pm 4.1$  nm (mean  $\pm$  SE,

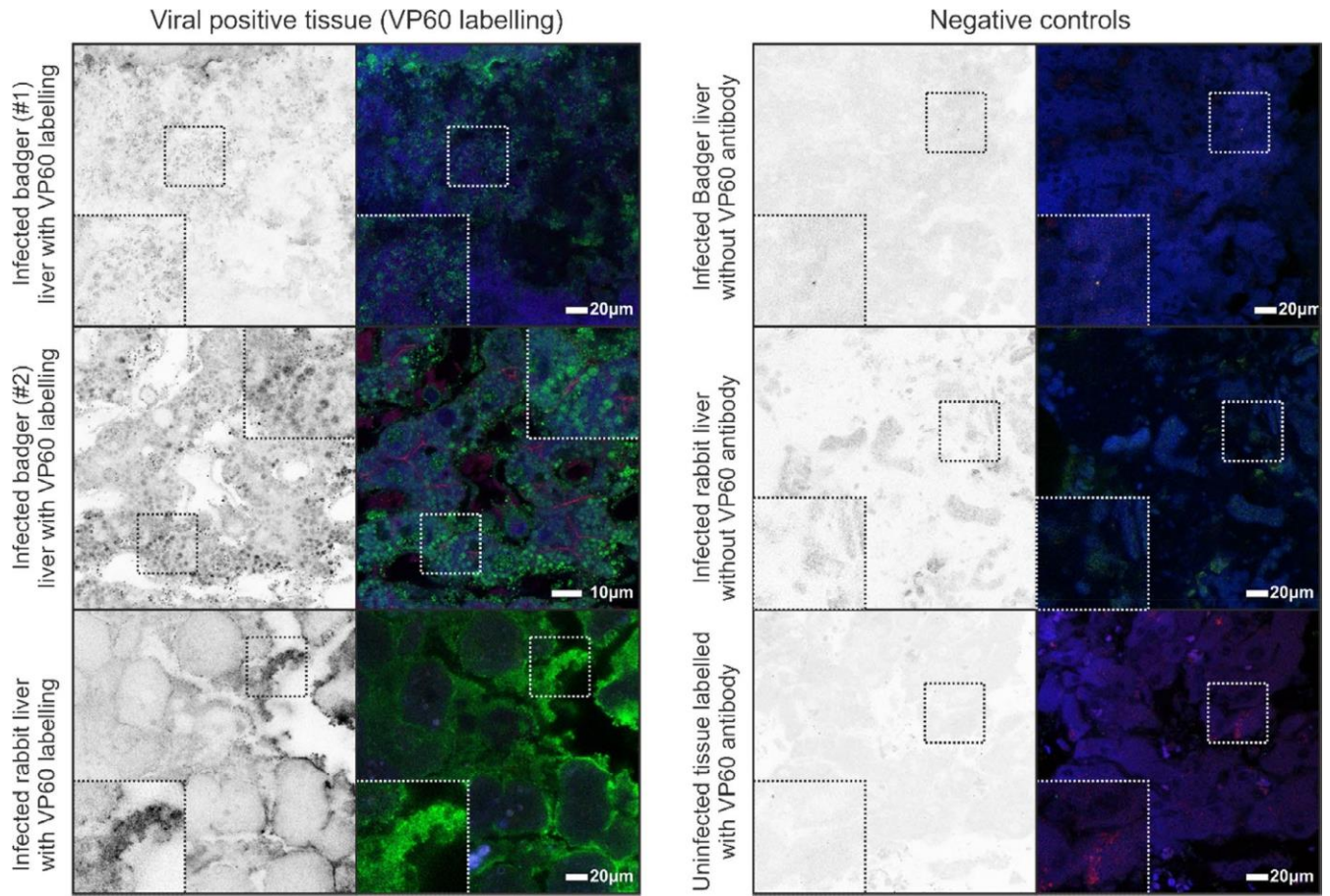


**FIGURE 13** Immunofluorescence using Virlab polyclonal antibody to detect viral protein (green), DAPI staining was used to detect DNA (blue) and phalloidin staining to detect actin filaments (red). Badger #1 (B5), badger #2 (B6). All the figures present the greyscale/inverted contrast at the left and the original view at the right

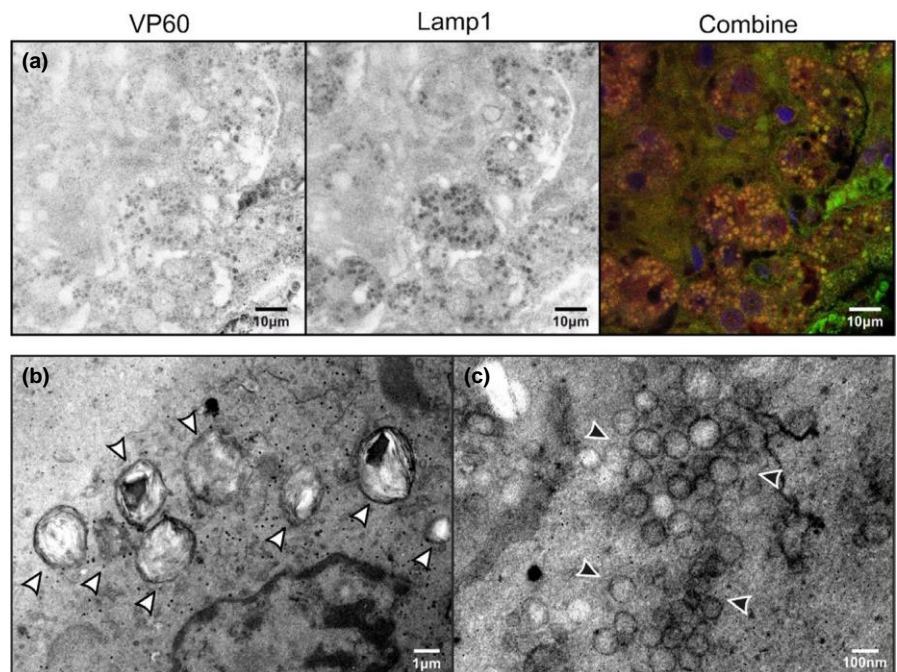


**FIGURE 14** Immunolabelling of viral protein VP60 (a-left, greyscale), LAMP 1 (a-middle, greyscale) and combined (a-right). (b) Transmission electron microscopy showing clusters of lysosomal like structures (white arrowheads) within hepatocytes of badger (B5). (c) Vesicles (black arrowheads) were also observed in the hepatocytes of badger B5

**TABLE 2** RT-qPCR amplification results and respective estimated viral loads per mg of tissue

Organs	Viral copies/mg tissue <sup>a</sup>									
	B1	B2	B3	B4	B5	B6	B7	B8	B9	B10
Liver	1.65 × 10 <sup>4</sup>	ND	ND	ND	2.99 × 10 <sup>6</sup>	1.14 × 10 <sup>4</sup>	1.69 × 10 <sup>5</sup>	2.84 × 10 <sup>4</sup>	2.09 × 10 <sup>5</sup>	6.02 × 10 <sup>5</sup>
Spleen	3.68 × 10 <sup>3</sup>	ND	ND	ND	4.25 × 10 <sup>5</sup>	1.66 × 10 <sup>6</sup>	5.53 × 10 <sup>5</sup>	3.34 × 10 <sup>4</sup>	5.01 × 10 <sup>5</sup>	1.92 × 10 <sup>5</sup>
Heart	7.13 × 10 <sup>4</sup>	ND	ND	ND	1.56 × 10 <sup>3</sup>	1.18 × 10 <sup>5</sup>	3.16 × 10 <sup>3</sup>	ND	8.14 × 10 <sup>2</sup>	4.57 × 10 <sup>3</sup>
Lungs	1.57 × 10 <sup>6</sup>	ND	ND	ND	1.21 × 10 <sup>6</sup>	5.15 × 10 <sup>3</sup>	5.78 × 10 <sup>2</sup>	1.19 × 10 <sup>3</sup>	1.67 × 10 <sup>3</sup>	ND
Duodenum	9.78 × 10 <sup>4</sup>	ND	ND	ND	3.31 × 10 <sup>3</sup>	4.75 × 10 <sup>5</sup>	7.47 × 10 <sup>4</sup>	5.50 × 10 <sup>3</sup>	8.67 × 10 <sup>3</sup>	1.75 × 10 <sup>4</sup>
Kidney	ND	ND	ND	ND	3.07 × 10 <sup>4</sup>	5.15 × 10 <sup>3</sup>	7.57 × 10 <sup>4</sup>	ND	5.63 × 10 <sup>2</sup>	8.90 × 10 <sup>3</sup>
Faeces	ND	ND	ND	ND	1.10 × 10 <sup>3</sup>	1.57 × 10 <sup>5</sup>	ND	ND	3.66 × 10 <sup>3</sup>	1.74 × 10 <sup>4</sup>
Mesenteric lymph node	NT	NT	NT	N	NT	NT	3.44 × 10 <sup>4</sup>	3.34 × 10 <sup>4</sup>	NT	NT

<sup>a</sup>According to the quantitative method described by Duarte et al. (2015). NT, not tested; ND, not detected; Darker cells correspond to higher viral loads.

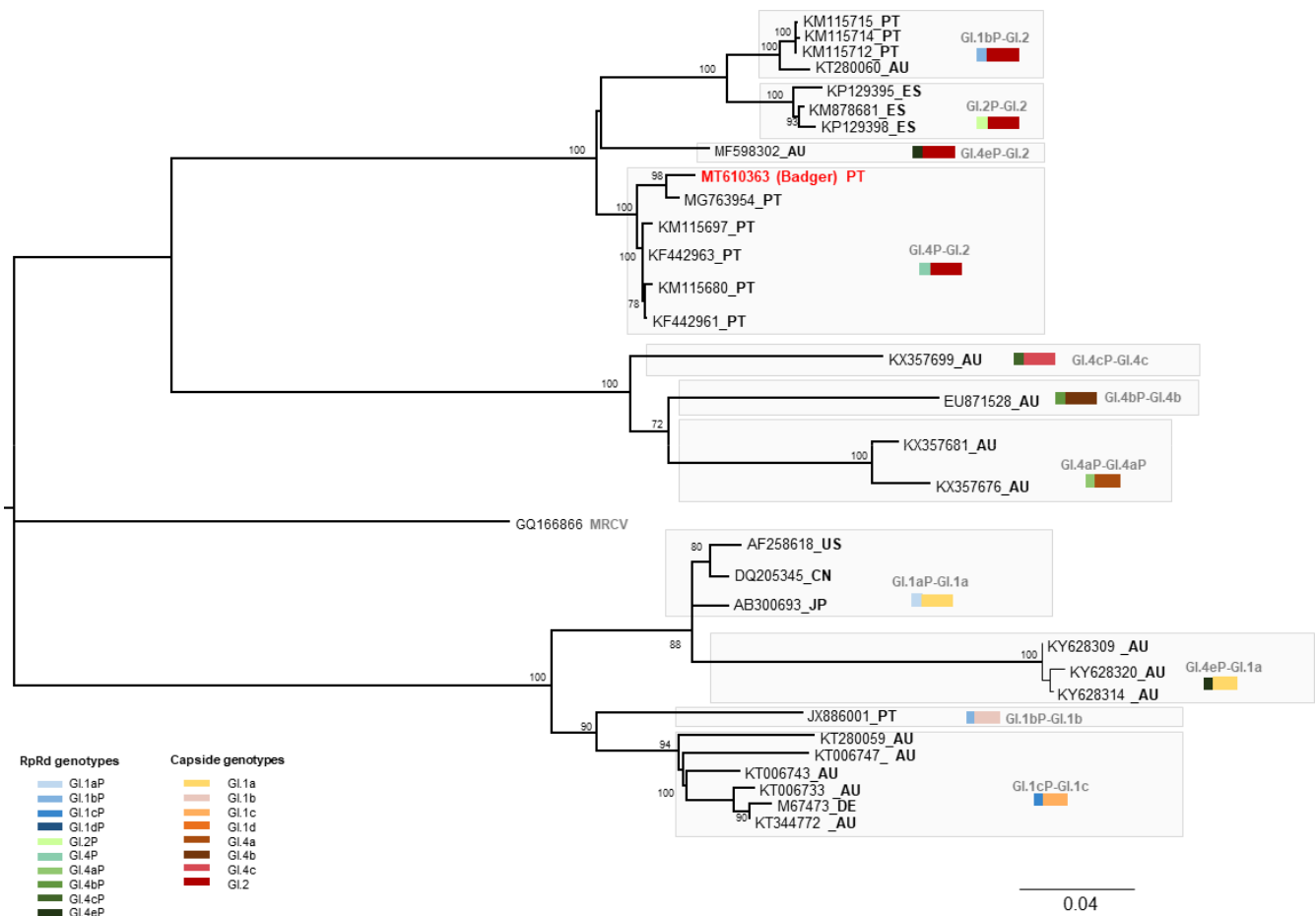


**FIGURE 15** Unrooted phylogenetic tree inferred by using the maximum likelihood method and general time reversible model (Nei & Kumar, 2000). The tree with the highest log likelihood (−13922.65) is shown. A discrete gamma distribution was used to model evolutionary rate differences among sites (5 categories (+G, parameter = 1.4546)). The rate variation model allowed for some sites to be evolutionarily invariable ([+I], 50.56% sites). The tree is drawn to scale, with branch lengths measured in the number of substitutions per site. This analysis involved 32 nucleotide sequences. Codon positions included were 1st + 2nd+3rd + non-coding. There were a total of 2,191 positions in the final dataset. The analyses were conducted in MEGA X (Kumar et al., 2018), and the tree was edited with FigTree software V1.4.4

30 measures, Figure 16) compatible with RHDV particles whose diameter range from 27 to 40 nm (Capucci et al., 1991; Ohlinger et al., 1990).

The virions were detected in the nucleus and cytoplasm of hepatocytes, in the hepatic interstitium, in the alveolar epithelial cells, in the heart myocytes, and in the cytoplasm of liver Kupfer cells. No

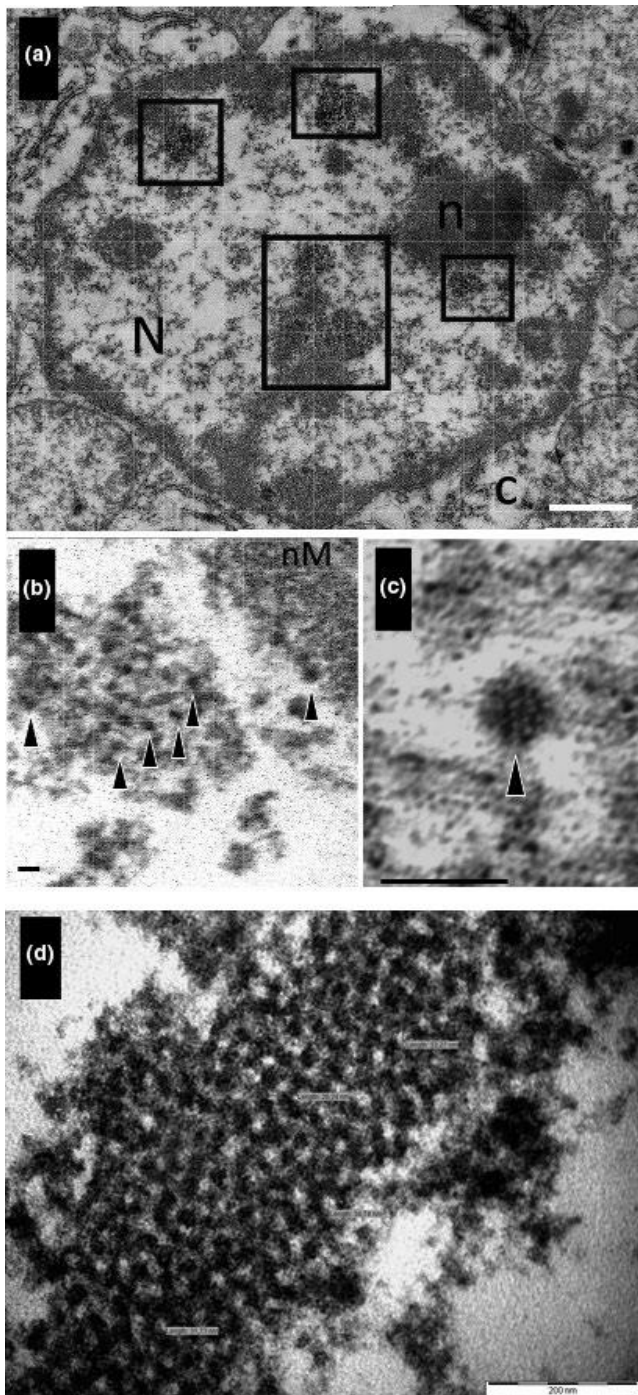


**FIGURE 16** Transmission electron micrographs of badger B5 liver. (a) Low magnification showing the nucleus (N) of an hepatocyte, with an eccentric nucleolus (n), with several clusters of viral particles (insets). (b) High magnification of the nucleus showing clusters of particles (arrow heads), which differ from neighbouring chromatin (c) adjacent to nuclear membrane (nM). (c) Detail of a viral particle (arrowhead) suggesting an octagonal shape. Bars: 1  $\mu\text{m}$  (white bar), 50 nm (black bar). (d) High magnification of an apparent intranuclear viral factory, with viral particles measuring from 26 to 38 nm, compatible with caliciviruses. Bar: 200 nm

virion-like structures were observed in a badger (unnumbered, used as negative control), that tested RHDV2-negative on the RT-qPCR.

### 3.8 | Virological analyses besides RHDV2

None of badgers B1, B5 to B10 was positive for all the other viruses tested.

### 3.9 | Bacteriological analysis

Low numbers of *Micrococcus* sp. and *Staphylococcus sciuri* were isolated from the liver and lung of badger B5. The remaining organs showed no aerobic or anaerobic bacterial growth.

Regarding badger B6, *Escherichia coli* was isolated from the liver and spleen, and low numbers of *Clostridium* sp. were isolated from the liver, spleen and kidney.

In the samples collected from badgers B7 and B8, low quantities of *Klebsiella oxytoca* and *Klebsiella pneumoniae* ssp. *pneumoniae* were isolated, respectively. No *Mycobacterium* spp. was detected in the badgers.

### 3.10 | Parasitological analysis

No ecto- or endoparasites were found in badgers B1, B7 and B8. In Badger B6, fleas were identified as *Pulex irritans*. For badgers B5 and B6, hookworm eggs were found through the flotation method. In the later, adult forms of hookworms (family Ancylostomatidae) were also detected during the analysis of the gastrointestinal content. *Isospora* spp., *Uncinaria criniformis* and nematodes from Capillariidae family were identified in badger B6, and *Capillaria* sp. in badger B10.

## 4 | DISCUSSION

Our work was conducted in the scope of a national surveillance programme for RHDV2 in wild rabbits and sympatric species (Action Plan for the Control of Rabbit Haemorrhagic Disease Virus, Dispatch 4757/17 of 30st May MAFDR). As sympatric species, European badgers were also included in the monitoring programme, which is why those found dead were sampled for investigation. However, the poor quality of these opportunistic biological samples poses major challenges to the laboratory diagnosis, overcome through the establishment of a comprehensive diagnosis strategy combining several molecular and antigen detection methods, sequencing analysis and electron microscopy observation. The serological investigation was not possible due to the lack of fresh blood samples.

The methodological strategy adopted for this study was as follows: tissue samples were firstly tested by RT-qPCR (Duarte et al., 2015) allowing the subsequent selection of the RHDV2 positive badgers for further analyses. Of these, only the badgers showing milder autolysis were elected for RHDV2 sequencing analysis, IHC and TEM. The exception was made for badger B1, the only material available for the first two years of this investigation, and for which, tissues were used for testing, despite severe autolysis.

To exclude the possibility of the microscopic lesions being a consequence of other infectious agents rather than RHDV2, samples were tested for additional pathogens. Several potential Eurasian badger viruses (canine distemper virus, canine and feline parvovirus, canine, feline and porcine coronaviruses, type A rotavirus, Ausjesky disease virus and other herpesviruses) were investigated by molecular methods in the appropriate tissues. All samples tested negative. Although Eurasian badgers can be susceptible to several pathogenic bacteria (Franzo et al., 2017; Judge et al., 2017; Sin et al., 2014; Wragg et al., 2011), the isolates identified in this study probably represent contaminants, as histopathological analysis did not show any bacteria in the tissues or tissue alterations that could be related with the bacterial species isolated. *Micrococcus* and *Staphylococcus* identified in badger B5 are common skin commensals of animals and humans, while *Clostridium* and *Escherichia coli*, identified in badger B6, belong to their intestinal microbiota (Quinn et al., 2011). Also, to the best of our knowledge, the first three genera have not yet been related to bacterial infections in *Meles meles*, while *E. coli* was reported in badgers' bronchoalveolar lavages (McCarthy et al., 2009).

The RHDV2 viral loads found in the tested organs (Table 2) ranged from  $1.19 \times 10^3$  to  $2.99 \times 10^6$ , despite kidney, heart and lungs tested negative in some badgers. These values were lower than the ones described for domestic and wild rabbit (Carvalho et al., 2017), but are compatible with a systemic infection, following the possible ingestion of RHDV2-positive rabbits. However, the mere passage of the virus through the gastrointestinal tract, without surpassing this barrier, would result in faeces and intestine and, at most, the mesenteric lymph nodes testing positive to RHDV2, while all the other organs would test negative. That was not the case since liver, lungs and spleen showed consistent and relatively high viral loads in several badgers.

Amplification and sequencing analysis of a 2,188-nt long fragment comprising part of the RdRp gene and the complete the VP60 gene, confirmed the presence of RHDV2-RNA in the tissues of badgers B5 and B6. Despite only partial sequences of the RdRp gene were obtained for badgers B1, B7, B8 and B9 (as summarized in Table S1), they also confirmed the RT-qPCR results, demonstrating unequivocally the presence of viral RNA in the badgers' tissues.

The molecular data was supported by the immunohistochemistry, immunofluorescence and dot blot results, alongside the gross pathology and histopathological lesions. Dot blot analysis of liver homogenates from badger B5 and B6 confirmed the presence of RHDV or RHDV2 protein in these organs. Curiously, the dot blot signal in B6 was stronger than in B5, despite the RT-qPCR results showed higher viral loads (deduced from the number of RNA copies) in B5 tissues. However, dot blot is not a quantitative technique and tissue homogenizations for dot blot were not carried out as accurately as for RNA extraction.

Gross pathology and histopathology suggest that multiorgan failure (heart, kidney and lung) could account for the proximal cause of death. The presence of iron deposits in the spleen, liver and lungs indicate haemorrhagic events, possibly due to chronic blood losses, more severe in the case of badgers B5 and B8, whose spleens were highly infiltrated with haemosiderin-laden macrophages. Although

liver necrosis in badgers was not as evident as normally seen in rabbits infected with RHDV2 (Abade dos Santos et al., 2017; Soliman et al., 2016; Umer et al., 2017), hepatocytes showed hydropic degeneration and individual cell necrosis. Another difference from rabbits is the lymphoid hyperplasia that was observed in three of four analysed badgers. This may indicate a more adjusted response to the viral infection, in accordance with the lower viral loads observed in the badgers, compared with rabbits.

Altogether, despite not so severe, the lesions observed may be accounted for a poor clinical evolution, leading to a moribund status incompatible with survival in the wild, taking into account that a weakened animal hardly survives, especially if it need to prey for food.

Additionally, the lower severity of the lesions compared to rabbits seems to indicate a less aggressive viral infection in this species. Despite different GI.2 strains showing different virulence were described, there is no data relating possible differences in the severity and type of lesions induced in rabbits with different strains. The pattern and severity of lesions may also change according to the clinical evolution, which in turn could vary due to intrinsic individual or species-related resistance and natural or acquired immunity to the infection. Nonetheless, if the course of the infection is less fulminating in badgers than in rabbits, probably because badger is not a usual host of this virus, it may favour the dissemination of RHDV2 in the wild as a disease with a longer course will allow virus excretion in the faeces for longer periods.

Finally, by transmission electron microscopy we demonstrated the presence of viral particles compatible with RHDV2 in several badgers' tissues. Despite the poor preservation condition of the tissues, viral factories were observed providing evidence of active replication of the virus in the cells. Furthermore, the observation of viral factories in the hepatocyte nucleus revealed, we believe that for the first time, the RHDV2 passage through the nucleus during replication. This observation had been previously reported in RHDV-infected hepatocytes by Marcato et al. (1991). The meaning of this finding is still unclear, given that a nuclear phase was not described in the replicative cycle of Caliciviridae, despite the presence of viral factories in the nucleus of infected cells was previously described in feline calicivirus infection (Pesavento et al., 2004). Regarding the present study, although the breakdown of the cell nuclear membrane may have allowed virions to pass into the nucleus as suggested before (Pesavento et al., 2004), since virions were exclusively grouped resembling viral factories, this scenario is unlikely. On the other hand, these clusters of virions within the nucleus were observed in several cells, where virions were not present in the cytoplasm. The presence of virions compatible with RHDV2 has already been observed by our team in the nucleus of hepatocyte cells from rabbits that died infected with RHDV2 (data not shown).

By immunofluorescence, we confirmed the presence of many lysosomes or autophagosome structures in the hepatocyte cytoplasm, containing mature virions (Figure 15). As previously described (Vallejo et al., 2014), after RHDV infection, the host cells initiate a rapid autophagic response that then declines, culminating in apoptosis. The vesicles shown in Figure 15 were also observed in RHDV-infected liver cells by these same authors.

During the +Coelho project, that operationalises the Action Plan, a total of 25 dead rabbits from the Santarém district were sampled between March 2017 and March 2020, of which 15 (60%) were positive for RHDV2.

To the best of our knowledge, no Lagoviruses had ever been described in wild badgers, in natural or experimental infections. In this study, we provide evidence that RHDV2 may have crossed another species barrier from the Leporidae family (order Lagomorpha) to the Mustelidae family (order Carnivora), a remarkable paradigm shift for the pathogenic potential of this virus.

More studies are now needed to understand whether these cases represent a set of individual spillover events or a true species jump. The detection of RHDV2 in badgers along three consecutive years (2017–2020) supports, in our opinion, the second scenario, but further investigations are necessary to confirm the geographic and temporal extension of this event.

Another future interesting study concerns the research of other calicivirus in this species, namely viruses close to non-pathogenic Lagoviruses, which may serve as donors of genetic material and thus contribute to the evolution of *Lagovirus europaeus* and the emergence of new pathogenic strains.

Experimental infections with European badgers would help to clarify the baseline level of susceptibility to infection; however, they are extremely complicated in protected species. Nonetheless, priority investigations should include further RHDV2 monitoring in badgers in the Santarém District as well as in other geographical areas, to clarify viral evolution within this host species, to evaluate the pathogenic impact of RHDV2 strains adapted to badgers towards rabbits and to understand the role of the Eurasian badger as a reservoir host for RHDV2.

## ACKNOWLEDGEMENTS

We thank Mr. Sebastião Miguel (Hunting manager) for field support, Dr. José Moura Nunes (Instituto Português de Oncologia, Lisboa) for guidance with the IHC test, Dr. Jacinto Gomes (INIAV IP, Head of Parasitology Lab) for the parasitological tests, Dr. Teresa Albuquerque and Dr. Mónica Cunha (INIAV I.P., Bacteriology Lab) for the bacteriological tests. We are thankful to the remaining team of the Department of Biochemistry and Molecular Biology of UniOvi, Spain, where some sequencing and dot blot were carried out. We thank also Mrs Sandra Carvalho and Mrs Maria do Rosário Luís (Anatomical Pathology Laboratory) for technical assistance, and Dr. Manuela Oliveira (Microbiology Laboratory) and Dr. Isabel Fonseca (Parasitology Laboratory) of the Faculty of Veterinary Medicine, University of Lisbon, for the access to the facilities.

## CONFLICT OF INTEREST

The authors declare no competing interests.

## AUTHORS' CONTRIBUTIONS

Abade dos Santos, F.A. contributed to conceptualization, investigation, methodology, resources and writing – original draft preparation. Pinto, A. contributed to formal analysis, investigation,

methodology and resources. Burgoyne, T. contributed to investigation and resources. Dalton, K.P. contributed to investigation, resources and validation. Carvalho C.L. contributed to investigation. Ramilo, D. contributed to investigation. Carneiro, C. contributed to investigation. Carvalho, T. contributed to investigation, and writing – review and editing. Peleteiro, M.C. contributed to funding acquisition, supervision, visualization, validation, writing – review and editing. Parra, F. contributed to conceptualization, funding acquisition, supervision, validation, writing – review and editing. Duarte, M.D. contributed to conceptualization, funding acquisition, investigation, project administration, supervision, validation and writing – review and editing.

## ETHICAL STATEMENT

This study did not use live animals and was carried out within the scope of a National Action Plan (Projects +Coelho1 and +Coelho 2, Dispatch no. 4757/2017 of 31 May), with the legal authorizations from the National Authority—the Institute for Nature Conservation and Forests (Instituto da Conservação da Natureza e das Florestas, I.P., ICNF).

## DATA AVAILABILITY STATEMENT

The data that support the findings of this study are available from the corresponding author upon reasonable request.

## ORCID

Fábio A. Abade dos Santos  <https://orcid.org/0000-0002-0696-7322>

Andreia Pinto  <https://orcid.org/0000-0002-0840-6844>

Thomas Burgoyne  <https://orcid.org/0000-0002-8428-720X>

Kevin P. Dalton  <https://orcid.org/0000-0002-7086-1979>

Carina L. Carvalho  <https://orcid.org/0000-0002-6648-9254>

David W. Ramilo  <https://orcid.org/0000-0003-4096-2581>

Tânia Carvalho  <https://orcid.org/0000-0002-5283-5013>

M. Conceição Peleteiro  <https://orcid.org/0000-0003-1848-558X>

Francisco Parra  <https://orcid.org/0000-0002-1885-9521>

Margarida D. Duarte  <https://orcid.org/0000-0003-1488-9659>

## REFERENCES

- Abade dos Santos, F. A., Carvalho, C., Nuno, O., Correia, J. J., Henriques, M., Peleteiro, M. C., Fevereiro, M., & Duarte, M. D. (2017). Detection of rabbit Haemorrhagic disease virus 2 during the wild rabbit (*Oryctolagus cuniculus*) eradication from the Berlengas archipelago, Portugal. *BMC Veterinary Research*, *13*, 336. <https://doi.org/10.1186/s12917-017-1257-3>
- Abrantes, J., Droillard, C., Lopes, A. M., Lemaitre, E., Lucas, P., Blanchard, Y., Marchandeu, S., Esteves, P. J., & Le Gall-Reculé, G. (2020). Recombination at the emergence of the pathogenic rabbit haemorrhagic disease virus Lagovirus europaeus/GI.2. *Scientific Reports*, *10*, 1–12. <https://doi.org/10.1038/s41598-020-71303-4>
- Downie T. (1990). *Theory and Practice of Histological Techniques* Edited by J.D. Bancroft & A. Stevens, Churchill Livingstone, Edinburgh, 740 pages, £55.00. *Histopathology*, *17*, (4), 1–740. <http://dx.doi.org/10.1111/j.1365-2559.1990.tb00755.x>
- Calvete, C., Mendoza, M., Sarto, M., Jiménez de Bagués, M. P., Luján, L., Molín, J., Calvo, A. J., Monroy, F., & Calvo, J. H. (2019). Detection

- of rabbit hemorrhagic disease virus GI. 2 / RHDV2 / B in the Mediterranean pine vole (*Microtus Duodecimcostatus*) and white-toothed shrew (*Crocidura russula*). *Journal of Wildlife Diseases*, 55, 1–6. <https://doi.org/10.7589/2018-05-124>
- Camarda, A., Pugliese, N., Cavadini, P., Circella, E., Capucci, L., Caroli, A., Legretto, M., Mallia, E., & Lavazza, A. (2014). Detection of the new emerging rabbit haemorrhagic disease type 2 virus (RHDV2) in Sicily from rabbit (*Oryctolagus cuniculus*) and Italian hare (*Lepus corsicanus*). *Research in Veterinary Science*, 97, 642–645. <https://doi.org/10.1016/j.rvsc.2014.10.008>
- Capucci, L., Fusi, P., Lavazza, A., Pacciarini, M. L., & Rossi, C. (1996). Detection and preliminary characterization of a new rabbit calicivirus related to rabbit hemorrhagic disease virus but nonpathogenic. *Journal of Virology*, 70, 8614–8623. <https://doi.org/10.1128/JVI.70.12.8614-8623.1996>
- Capucci, L., Scicluna, M., & Lavazza, A. (1991). Diagnosis of viral haemorrhagic disease of rabbits and the European brown hare syndrome. *Revue Scientifique et Technique*, 10, 347–370. <https://doi.org/10.20506/rst.10.2.561>
- Carvalho, C. L., Duarte, E. L., Monteiro, M., Botelho, A., Albuquerque, T., Fevereiro, M., Henriques, A. M., Barros, S. S., & Duarte, M. D. (2017). Challenges in the rabbit haemorrhagic disease 2 (RHDV2) molecular diagnosis of vaccinated rabbits. *Veterinary Microbiology*, 198, 43–50. <https://doi.org/10.1016/j.vetmic.2016.12.006>
- Chiari, M., Molinari, S., Cavadini, P., Bertasi, B., Zanoni, M., Capucci, L., & Lavazza, A. (2016). Red foxes (*Vulpes vulpes*) feeding brown hares (*Lepus europaeus*) infected by European brown hare syndrome virus (EBHSV) might be involved in the spread of the virus. *European Journal of Wildlife Research*, 62(6), 761–765. <https://doi.org/10.1007/s10344-016-1055-4>
- Dalton, K. P., Arnal, J. L., Benito, A. A., Chacón, G., Martín Alonso, J. M., & Parra, F. (2018). Conventional and real time RT-PCR assays for the detection and differentiation of variant rabbit hemorrhagic disease virus (RHDVb) and its recombinants. *Journal of Virological Methods*, 257, 118–122. <https://doi.org/10.1016/j.jviromet.2017.10.009>
- Di Profio, F., Melegari, I., Sarchese, V., Robetto, S., Bermudez Sanchez, S., Carella, E., Orusa, R., Cavadini, P., Lavazza, A., Marsilio, F., Martella, V., & Di Martino, B. (2017). Potential role of wolf (*Canis lupus*) as passive carrier of European brown hare syndrome virus (EBHSV) Research in Veterinary Science Potential role of wolf (*Canis lupus*) as passive carrier of European brown hare syndrome virus (EBHSV). *Research in Veterinary Science*, 117, 81–84. <https://doi.org/10.1016/j.rvsc.2017.11.016>
- Duarte, M. D., Carvalho, C. L., Barros, S. C., Henriques, A. M., Ramos, F., Faguhla, T., Luís, T., Duarte, E. L., & Fevereiro, M. (2015). A real time Taqman RT-PCR for the detection of rabbit hemorrhagic disease virus 2 (RHDV2). *Journal of Virological Methods*, 219, 90–95. <https://doi.org/10.1016/j.jviromet.2015.03.017>
- Fedriani, J. M., Palomares, F., & Delibes, M. (1999). Niche relations among three sympatric Mediterranean carnivores. *Oecologia*, 121, 138–148. <https://doi.org/10.1007/s004420050915>
- Franzo, G., Massi, P., Tucciarone, C. M., Barbieri, I., Tosi, G., Fiorentini, L., Ciccozzi, M., Lavazza, A., Cecchinato, M., & Moreno, A. (2017). Think globally, act locally: Phylodynamic reconstruction of infectious bronchitis virus (IBV) QX genotype (GI-19 lineage) reveals different population dynamics and spreading patterns when evaluated on different epidemiological scales. *PLoS One*, 12, 1–20. <https://doi.org/10.1371/journal.pone.0184401>
- González, A. M. (2019). Caracterización antigénica y diseño de vacunas frente a la nueva variante del virus de la enfermedad hemorrágica del conejo. PhD thesis. University of Oviedo.
- Judge, J., Wilson, G. J., Macarthur, R., McDonald, R. A., & Delahay, R. J. (2017). Abundance of badgers (*Meles meles*) in England and Wales. *Scientific Reports*, 7, 1–8. <https://doi.org/10.1038/s41598-017-00378-3>
- Kumar, S., Stecher, G., Li, M., Knyaz, C., & Tamura, K. (2018). Molecular evolutionary genetics analysis across computing platforms. *Molecular Biology and Evolution*, 35(6), 1547–1549.
- Le Gall-Recule, G., Zwingelstein, F., Boucher, S., Le Normand, B., Plassiart, G., Portejoie, Y., Decors, A., Bertagnoli, S., Guerin, J.-L., & Marchandeau, S. (2011). Detection of a new variant of rabbit haemorrhagic disease virus in France. *The Veterinary Record*, 168, 137–138. <https://doi.org/10.1136/vr.d697>
- Le Gall-Reculé, G., Zwingelstein, F., Fages, M. P., Bertagnoli, S., Gelfi, J., Aubineau, J., Roobrouck, A., Botti, G., Lavazza, A., & Marchandeau, S. (2011). Characterisation of a non-pathogenic and non-protective infectious rabbit lagovirus related to RHDV. *Virology*, 410, 395–402. <https://doi.org/10.1016/j.virol.2010.12.001>
- Le Pendu, J., Abrantes, J., Bertagnoli, S., Guitton, J.-S., Le Gall-Reculé, G., Lopes, A. M., Marchandeau, S., Alda, F., Almeida, T., Célio, A. P., Bárcena, J., Burmakina, G., Blanco, E., Calvete, C., Cavadini, P., Cooke, B., Dalton, K., Delibes Mateos, M., Deptula, W., ... Esteves, P. (2017). Proposal for a unified classification system and nomenclature of lagoviruses. *Journal of General Virology*, 98, 1658–1666. <https://doi.org/10.1099/jgv.0.000840>
- Liu, S., Xue, H., Pu, B., & Qian, N. (1984). A new viral disease in rabbit. *Animal Husbandry & Veterinary Medicine*, 16, 253–255.
- Lopes, A. M., Marques, S., Silva, E., Magalhães, M. J., Pinheiro, A., Alves, P. C., Le Pendu, J., Esteves, P. J., Thompson, G., & Abrantes, J. (2014). Detection of RHDV strains in the Iberian hare (*Lepus granatensis*): Earliest evidence of rabbit lagovirus cross-species infection. *Veterinary Research*, 45, 1–7. <https://doi.org/10.1186/s13567-014-0094-7>
- Mahar, J. E., Hall, R. N., Peacock, D., Kovaliski, J., Piper, M., Mourant, R., & Huang, N. (2018). Rabbit hemorrhagic disease virus 2 (RHDV2; GI.2) is replacing endemic strains of RHDV in the Australian landscape within 18 months of its arrival. *Journal of Virology*, 2, 1–15. <https://doi.org/10.1128/JVI.01374-17>
- Marcato, P., Benazzi, C., Vecchi, G., Galeotti, M., Della Salda, L., Sarli, G., & Lucidi, P. (1991). Clinical and pathological features of viral haemorrhagic disease of rabbits and the European brown hare syndrome. *Revue Scientifique et Technique*, 10, 371–392.
- McCarthy, G., Shiel, R., O'Rourke, L., Murphy, D., Corner, L., Costello, E., & Gormley, E. (2009). Bronchoalveolar lavage cytology from captive badgers. *Veterinary Clinical Pathology*, 38, 381–387. <https://doi.org/10.1111/j.1939-165X.2009.00127.x>
- Meyers, G., Wirblich, C., & Thiel, H. J. (1991). Rabbit hemorrhagic disease virus-molecular cloning and nucleotide sequencing of a calicivirus genome. *Virology*, 184, 664–676. [https://doi.org/10.1016/0042-6822\(91\)90436-F](https://doi.org/10.1016/0042-6822(91)90436-F)
- Mutze, G., Bird, P., Kovaliski, J., Peacock, D., Jennings, S., & Cooke, B. (2002). Emerging epidemiological patterns in rabbit haemorrhagic disease, its interaction with myxomatosis, and their effects on rabbit populations in South Australia. *Wildlife Research*, 29, 577–590. <https://doi.org/10.1071/WR00100>
- Nei, M., & Kumar, S. (2000). *Molecular evolution and phylogenetics*. New York: Oxford University Press.
- Neimanis, A. S., Ahola, H., Pettersson, U. L., Lopes, A. M., Abrantes, J., Zohari, S., Esteves, P. J., & Gaviera-widén, D. (2018). Overcoming species barriers: An outbreak of Lagovirus europaeus GI. 2 / RHDV2 in an isolated population of mountain hares (*Lepus timidus*). *BMC Veterinary Research*, 1–12.
- Ohlinger, V. F., Haas, B., Meyers, G., Weiland, F., & Thiel, H.-J. (1990). Identification and characterization of the virus causing rabbit hemorrhagic disease. *Journal of Virology*, 64, 3331–3336.
- OIE. (2019). *Rabbit haemorrhagic disease (Technical disease card)* (pp. 1–7). World Organisation for Animal Health [https://www.oie.int/fileadmin/Home/eng/Animal\\_Health\\_in\\_the\\_World/docs/pdf/Disease\\_cards/RHD.pdf](https://www.oie.int/fileadmin/Home/eng/Animal_Health_in_the_World/docs/pdf/Disease_cards/RHD.pdf).

- Peleteiro, M. C., Ferreira da Silva, J., Dias-Pereira, P., Carvalho, T., Faustino, A., Correia, J., Pissarra, H., & Stilwell, G. (2016). *Manual de Necropsia Veterinária 1a*. (Lidel, Ed.). Lisboa.
- Pesavento, P. A., Maclachlan, N. J., Dillard-Telm, L., Grant, C. K., & Hurley, K. F. (2004). Pathologic, immunohistochemical, and electron microscopic findings in naturally occurring virulent systemic feline calicivirus infection in cats. *Veterinary Pathology*, *41*, 257–263. <https://doi.org/10.1354/vp.41-3-257>
- Puggioni, G., Cavadini, P., Maestrone, C., Scivoli, R., Botti, G., Ligios, C., Le Gall-Reculé, G., Lavazza, A., & Capucci, L. (2013). The new French 2010 Rabbit Hemorrhagic Disease Virus causes an RHD-like disease in the Sardinian Cape hare (*Lepus capensis mediterraneus*). *Veterinary Research*, *44*, 1–7. <https://doi.org/10.1186/1297-9716-44-96>
- Quinn, P., Markey, B., Leonard, F., Hartigan, P., Fanning, S., & Fitzpatrick, E. (2011). Animal diversity, natural history and conservation – Volume 22nd Edition. In L. M. Rosalino, T. Sales-Luis, M. Pinto Basto, N. M. Pedroso, L. Tavares, C. L. Vilela, & M. Oliveira (Eds.), *Veterinary microbiology and microbial disease* (pp. 1–17). Wiley-Blackwell.
- Silvério, D., Lopes, A. M., Melo-ferreira, J., Magalhaes, M. J., Ponterroso, P., Serronha, A., Maio, E., Alves, P. C., Esteves, P. J., & Abrantes, J. (2018). Insights into the evolution of the new variant rabbit haemorrhagic disease virus (GI. 2) and the identification of novel recombinant strains. *Transboundary and Emerging*, *00*, 1–10. <https://doi.org/10.1111/tbed.12830>
- Sin, Y. W., Annavi, G., Dugdale, H. L., Newman, C., Burke, T., & MacDonald, D. W. (2014). Pathogen burden, co-infection and major histocompatibility complex variability in the European badger (*Meles meles*). *Molecular Ecology*, *23*, 5072–5088. <https://doi.org/10.1111/mec.12917>
- Soliman, M., Rhaman, M., Samy, M., Mehana, O., & Nasef, S. (2016). Molecular, clinical and pathological studies on viral rabbit hemorrhagic disease. *Alexandria Journal of Veterinary Science.*, *48*, 20. <https://doi.org/10.5455/ajvs.207505>
- Strive, T., Wright, J. D., & Robinson, A. J. (2009). Identification and partial characterisation of a new lagovirus in Australian wild rabbits. *Virology*, *384*, 97–105. <https://doi.org/10.1016/j.virol.2008.11.004>
- Umer, F., Riasat, W. U., Asma, L., Aamer, B. Z., Javid, I. D., & Hamid, I. (2017). Gross pathological findings of rabbit hemorrhagic disease ( RHD ) in two (02) cases case report gross pathological findings of rabbit hemorrhagic disease ( RHD ) in two. *Research Journal for Veterinary Practitioners*, *1*(4), 39–40.
- USDA. (2020). Emerging risk notice. Rabbit Hemorrhagic Disease Virus, Type 2.
- Vallejo, D., Crespo, I., San-Miguel, B., Álvarez, M., Prieto, J., Tuñón, M. J., & González-Gallego, J. (2014). Autophagic response in the Rabbit Hemorrhagic Disease, an animal model of virally-induced fulminant hepatic failure. *Veterinary Research*, *45*, 1–13. <https://doi.org/10.1186/1297-9716-45-15>
- Velarde, R., Cavadini, P., Neimanis, A., Cabezón, O., Chiari, M., Gaffuri, A., Lavín, S., Grilli, G., Gavier-Widén, D., Lavazza, A., & Capucci, L. (2017). Spillover events of infection of brown hares (*Lepus europaeus*) with rabbit haemorrhagic disease type 2 virus (RHDV2) caused sporadic cases of an European brown hare syndrome-like disease in Italy and Spain. *Transboundary and Emerging Disease*, *64*, 1750–1761. <https://doi.org/10.1111/tbed.12562>
- Wragg, P. N., Strugnell, B. W., Whatmore, A. M., & Foster, G. (2011). Arcanobacterium haemolyticum in a badger (*Meles meles*). *Journal of Veterinary Diagnostic Investigation*, *23*, 1234–1235. <https://doi.org/10.1177/1040638711425585>

## SUPPORTING INFORMATION

Additional supporting information may be found online in the Supporting Information section.

---

**How to cite this article:** Abade dos Santos FA, Pinto A, Burgoyne T, et al. Spillover events of rabbit haemorrhagic disease virus 2 (recombinant GI.4P-GI.2) from Lagomorpha to Eurasian badger. *Transbound Emerg Dis*. 2021;00:1–16. <https://doi.org/10.1111/tbed.14059>

---